

Domain Decomposition Algorithm and Analytical Simulation of Coupled Flow in Reservoir / Well System

Richard Ewing, Akif Ibragimov, Raycho Lazarov
Institute for Scientific Computations, Texas A and M University , College Station,
Alexander Necrasov Institute of Mining Technology, Freiburg.

*Institute for Scientific Computation
Texas AandM University
College Station, TX 77843-3404*

Abstract. A model and analytical method for solving a problem of coupled fluid flow in the reservoir/well system is presented. The 3-D drainage area is composed of three connected media: the tubing, the annuli (considered as a super conducting collector), and the reservoir itself. To couple the fluid flows in these areas a non-overlapping Dirichlet-Neumann domain decomposition method is developed theoretically and tested numerically. The method allows to build an analytical hybrid simulator for accurate evaluation of the impact of the main geometrical and hydrodynamic parameters of the 3-D system on the pressure drop along the horizontal well and on its production index.

1. INTRODUCTION

The modern technology in oil and gas recovery requires new models and computational methods and techniques which take into account geometrical and hydrodynamics parameters of “small” perturbation. Mostly, this issue reflects the increasing understanding of the reservoir’s structure and geometry which make effective the usage of the so called “smart” technology [17]. Many presentations on the recent conference ”Horizontal Technology” [28] showed that the technological progress of horizontal well drilling has been recognized by the petroleum industry as a most efficient technique for reservoir development and characterization. A distinct property of horizontal wells is a bounded perforation with significant length in productive layer. At the same time, it is clear that a high span of perforation of the horizontal well may result in a significant pressure drop along the well-bore [2, 10, 16, 24, 20, 30, 21, 22, 23, 25]. The mechanics of pressure drop is very complex and is due to various factors, such as completion of the well, operation conditions (e.g. sand factor), the character of fluid flow inside the horizontal well and in the reservoir, geometry of the reservoir, hydrodynamic characteristic of the porous media, etc. These factors may lead to substantial decrease of well/reservoir conductivity ratio. The pressure drop results in stabilization of the well productivity; that is, beginning with a certain critical value, further extenuation of the wellbore’s length does not cause any increase

of productivity [8, 10, 24, 25]. It has been noted [2, 19, 21, 22, 23, 25] that for an accurate evaluation of the pressure drop along the well a coupled well-bore/reservoir flow model has to be considered. It has been shown [2] that in a 3-D unbounded reservoir with permeability less than 1-Darcy and laminar well flow the pressure drop along the well-bore is insignificant. This fact is related to the assumption that conductivity of the well in case of Poiseuille's flow is much higher than the conductivity in the reservoir and therefore, the pressure along the well changes weakly. At the same time, the data observed in multiple operating horizontal wells showed that productivity of these wells does not increase proportionally to the length. In recent papers (see, e.g. [21, 22, 23, 25]) this effect has been estimated by friction of the wall and acceleration terms in balance equation. In the present paper a model of a reservoir/well system composed of a tube of small radius with extremely high (infinite) conductivity, an intermediate annular zone with high but finite permeability, and the reservoir itself with low (less than 1 Darcy) permeability (see, Figure 1) is studied. In the physical sense the model we use takes into account the following phenomena:

- fluid flow inside tubing of the well,
- fluid flow in a screen and sand pack considered as one media with its own permeability and
- fluid flow in a bounded reservoir limited by top, bottom and external boundaries.

This embedded coupled model allows us to take into account the main parameters that produce pressure drop along the horizontal well. In practice the reservoir's and well's geometrical parameters are incomparable. Therefore, the combined impact of these parameters on coupled fluid flow inside the well and in the reservoir could not be efficiently estimated by methods of numerical analysis based on finite difference (finite element, etc.) approximation of governing equations. Our goal is to accurately evaluate the impact on well performance of the parameters of: (1) the geometry of the reservoir/well system, and (2) the hydrodynamic characteristic of fluid flow in three linked media (well, near well zone, and main part of the reservoir). For this purpose two analytical models are proposed. The first approach is based on the presentation of the reservoir pressure distribution in the form of convolution of a Green function of boundary problem with mixed type (Dirichlet and Neumann) of boundary conditions and with unknown density. For an explicit construction of the Green function, an alternating Schwartz algorithm is proposed and studied. This algorithm produces a sequence of solutions to a Dirichlet problem in a bigger (auxiliary) domain so that their restrictions to the original domain tends to the Green function of a mixed problem. Further discrete density is modeled by means of special coupling conditions on the wall of the well. A second approach is based on methods of separation of variables, which allows us to reduce the initial problem to the problem of computation the Fourier and Fourier Bessel coefficients on the boundaries of a cylindrical domain. The first approach accounts more precisely for the "global parameters" of the well/reservoir system such as size of the drainage zone, shape factors of the external boundary, of the reservoir, well's length etc. the second approach is aimed at accurate and explicit evaluation of the impact of the "local" geometrical and hydrodynamic parameters: tubing/casing "diameter", well /reservoir conductivity ratio etc., on the pressure distribution and production index.

It is very important to note that direct application of these methods is not feasible (impossible). Therefore, special domain decomposition algorithms are developed. We also must note that for convenience, these two approaches are presented in the paper separately and are applied to different domains. The paper is organized as follows: In Section 2 we present the coupled model of a well/reservoir system and discuss methods for an approximate solution. In Section 3 we construct an approximation of the Green function that is an important building

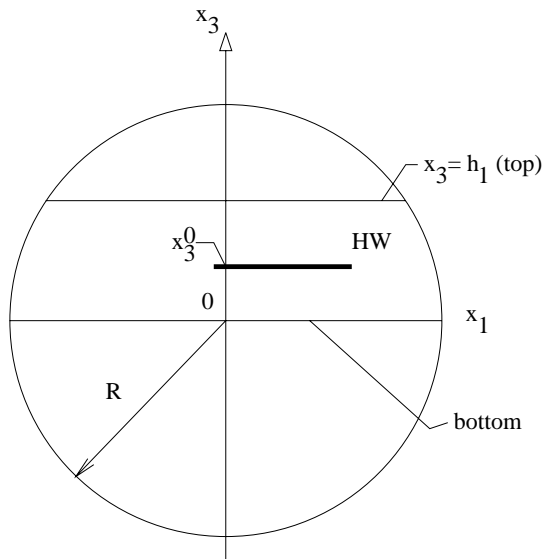


FIGURE 1. Reservoir/Well model

block in the numerical solution method. Further, in Section 4 we discuss the numerical implementation of the method and the computational results. Finally, in Section 5 we present and discuss a non-overlapping Schwartz algorithm in a non-homogeneous domain. In this section we present an explicit form of the solution and discuss the convergence of the corresponding iterative method for the Fourier-Bessel coefficients.

2. COUPLED FLOW MODEL

In this section we present a mathematical model of coupling two single-phase fluid flows: one inside a cylindrical well of finite length and another one in a bounded homogeneous porous media (called reservoir). We assume that inside the well the flow is steady-state, inertia-less, and governed by Stokes equations. The flow in the reservoir obeys Darcy's law. The well is assumed to be cased with very dense perforations uniformly distributed over its surface. At the interface between the well and the reservoir we use a coupling condition, introduced by Panfilov [26], that expresses a conservation of mass through the interface. The reservoir's filtration is in the radial direction to the interface of the well bore, while the inflow flux can be considered to be continuous across the surface.

2.1. Mathematical Model. In order to formulate the model we first introduce some necessary notations. The points in the 3-dimensional space R^3 are denoted by $x = (x_1, x_2, x_3)$. The reservoir is considered to be a spherical layer with thickness equal h :

$$\Omega \equiv B \cap \{x : 0 < x_3 < h\} \subset R^3,$$

where $B \equiv B(0, R) = \{x : |x| < R\}$ is a ball in R^3 with a center at the origin, and $|x|$ is the Euclidean length of x . The well W is a cylindrical cavity along the x_1 axes of constant radius r_w and finite length L , i.e.

$$W \equiv \{x : 0 < x_1 < L, x_2^2 + (x_3 - x_3^0)^2 < r_w^2\}, \text{ (see, Figure 1)}$$

It is assumed that:

1. The fluid is incompressible and filtration of flow in the porous media is governed by Darcy's law and the equation of continuity:

$$\vec{w} \equiv (w_1, w_2, w_3) = -\frac{K}{\mu} \nabla p, \quad \nabla \cdot \vec{w} = 0.$$

Here \vec{w} is vector velocity of fluid filtration and p is the reservoir pressure, K generally is a symmetrical tensor of permeability with measurable and bounded coefficients, and the μ is fluid viscosity. We assume that the porous media is isotropic and homogeneous and the fluid viscosity is constant. Substituting the expression for the velocity into the equation of continuity we obtain:

$$(1) \quad \Delta p = 0 \quad \text{in } \Omega \setminus W.$$

2. The following boundary conditions are satisfied on the boundary of the 3-D spherical layer (see, Figure 1) :

at the top ($x_3 = h$) and the bottom ($x_3 = 0$) of the reservoir no-flow conditions are prescribed, while the pressure p is specified on the external boundary $\Gamma_1 \equiv \{x : |x| = R, 0 < x_3 < h\}$ of the reservoir.

3. Inside the well we use a simplified model derived in [26] in terms of the averaged pressure and velocity over the a cross-section of the well. Let $D(x_1) = \{x : x_2^2 + (x_3 - x_3^0)^2 \leq r_w^2\}$ be a cross section W by a plane orthogonal to the axes x_1 at the point $(x_1, 0, x_3^0)$, and let $S(x_1)$ its boundary

$$(2) \quad S(x_1) \equiv \partial D(x_1) = \{(x_1, x_2, x_3) : x_2 = r_w \cos \phi, x_3 = x_3^0 + r_w \sin \phi, 0 \leq \phi < 2\pi\}.$$

Next, denote by $P_a(x_1)$ the average pressure in the well-bore over the disk $D(x_1)$ and by $V_1(x_1)$ the average component of the velocity of the flow over $D(x_1)$ the x_1 . It has been shown that under certain assumptions [26] the fluid flow inside the well W is governed by the following two equations:

$$(3) \quad V_1'(x_1) = -\frac{2}{r_w} w_r(x_1), \quad -\frac{1}{\mu} P_a'(x_1) = \frac{8}{r_w^2} V_1(x_1) + \frac{2}{r_w} w_r'(x_1).$$

Here $w_r(x_1)$ is the average over $S(x_1)$ of the trace of the radial component of the velocity, namely

$$(4) \quad w_r(x_1) = -\frac{K}{\mu} \int_{S(x_1)} \frac{\partial p}{\partial n} ds,$$

where n is outward normal unit vector to $S(x_1)$. Note, that in our case $\frac{\partial p}{\partial n} = \frac{\partial p}{\partial r}$ so that the notation $w_r(x_1)$ is justified.

4. The radius of the well is more than a hundreds times smaller than the other linear sizes of the well/reservoir system. That makes it possible to assume that we can neglect the dependence upon the angular variable ϕ of the trace of the reservoir pressure and the normal component of the velocity on $S(x_1)$ (defined by (2)). Therefore, we can use the notation

$$p(x_1, x_2, x_3)|_{S(x_1)} = \bar{p}(x_1).$$

5. The well pressure is specified as a given P_w constant for $x_1 = 0$. This end of the well is called dominated. The opposite end of the well, the point $x_1 = L$, is called a free end. At this end we specify the average velocity V_1 which expresses a balance of mass. This will lead to the following boundary conditions:

$$(5) \quad P_a(0) = P_w, \quad V_1(L) = \frac{1}{\pi r_w^2} \int_{D(L)} w_1(L, x_2, x_3) dx_2 dx_3.$$

6. The solution inside the well is completely specified by its boundary conditions while the solution in the reservoir is specified only on the top ($x_3 = h$), bottom ($x_3 = 0$) and external boundary Γ_1 . These two problems, called inner and external, are coupled via a condition on the well's interface. In this paper we will follow the scheme described in [2, 11, 19, 26]. For another approach for coupling external and internal problem we refer to [22, 25].

On the interface between the porous media and the well the pressure is continuous, while the velocities are allowed to be discontinuous. In [26] it has been shown that in this case the average pressure $P_a(x_1)$ in the well and the average of the trace of pressure in the reservoir $\bar{p}(x_1)$ on $S(x_1)$ satisfy the following interface condition:

$$(6) \quad \bar{p}(x_1) = P_a(x_1) + \frac{\mu}{2r_w}(r_w^2 w_r''(x_1) - 4w_r(x_1)).$$

The governing equation (3) in the well bore W and the conjugate condition (6) have been obtained in [26] for Stokes flow by averaging over the well bore cross section. The solution of the Stokes equations written in the cylindrical coordinate system was sought in the form of a power series with unknown coefficient depending on x_1 determined from the coupling conditions.

2.2. Decomposition of the initial problem. Here we propose an iterative method that reduces the problem of coupling flows in the reservoir (outer flow) and in the well (inner flow) by the condition (6) on the well/reservoir interface.

We propose the following iterative scheme:

1. Solve the outer boundary value problem in the reservoir with a given linear distribution P_0 on the well surface; as a result we find: (1) the pressure function $p(x)$ in the reservoir, (2) the average of the traces of the normal component $w_r(x_1)$ of velocity on the lateral surface of the well, and (3) the normal component $w_1(L, x_2, x_3)$ of the velocity on the free end of the well.
2. Using the $w_r(x_1)$ and $w_1(L, x_2, x_3)$ obtained, solve the inner problem (3), (5) in W ; as result the average pressure distribution $P_a(x_1)$ in the well is computed.
3. Solve

$$(7) \quad \Delta p = 0 \quad \text{in } \Omega \setminus W.$$

with boundary conditions (6) on the interface $S(x_1)$ and the following boundary conditions on the reservoir's boundary:

$$(8) \quad p_{x_3} = 0 \quad \text{for } x_3 = 0, h, \quad p(x) = p_R \quad \text{on } \Gamma_1.$$

4. Repeat steps 2 and 3 of this process until convergence.

2.3. Solution methods for the outer problem. Without loss of generality we can assume that $p_R = 0$. Let $G(x, \xi)$ be the Green's function of the mixed problem (6) – (8). By applying the theory of Newton's potential, the pressure function $p(x)$ can be represented in the form:

$$(9) \quad p(x) = \int_W G(x, \xi) \beta(\xi) d\xi, \quad x \in R^3$$

A classical way to obtain the unknown potential density $\beta(\xi)$ is: to substitute the potential $p(x)$ into the boundary condition (6) (where $P_a(x_1)$ is defined from the iteration procedure) and to solve the resulting integral equation. The numerical realization of this approach is well understood, but extremely expensive since it results in a boundary element method over a surface in 3-D.

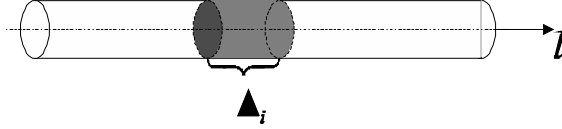


FIGURE 2. The well model

Under the assumption 4 in Section 2.1 we can substantially simplify the solution of the problem (6) – (8). Namely, we take the density as a function of the ξ_1 - variable and the singularity of the Green's function $G(x, \xi)$ is located along the axis x_1 . This allows us to use the following approximate construction:

1. Replace the well W (see, Figure 2 as a sum of a finite number of intervals on the axes x_1 defined by the points $0 = \xi_{1,0} < \xi_{1,1} < \dots < \xi_{1,N} = L$;
2. Approximate the potential (9) by taking β as piecewise constant over this partition so that

$$(10) \quad p(x) = \sum_1^N \beta_i \int_{\Delta_i} G(x, \xi), d\xi_1, \text{ where } , \Delta_i = [\xi_{1,i}, \xi_{1,i+1}];$$

3. Find the unknown discrete density $(\beta_1, \dots, \beta_N)$ by taking the equation (6) at the collocation points $(x_{1,j}, r_w, 0)$:

$$(11) \quad p(x_1, x_2, x_3) = P_a(x_1) + \frac{\mu}{2r_w}(r_w^2 w_r''(x_1) - 4w_r(x_1)).$$

Here $x_{1,j} \in \Delta_j$ is a specific point aimed to minimize the error of the quadrature formula.

Obviously, the main issue in applying this modification of the boundary element method is an explicit construction of the Green function $G(x, \xi)$. In an unbounded reservoir ($R = \infty$) of finite thickness h the function $G(x, \xi)$ is a superposition of an infinite number of fundamental solutions of Laplace equation [18]. These series does not converge. In case of a bounded domain such as parallelepiped or cylinder, the Green's function with Dirichlet condition on the side of this domain can be represented as a superposition of the source functions, but this series converge very slowly [7]. To overcome this difficulty, an iterative method for construction of Green's function has been developed in [13, 14]. Here we apply this approach for mixed boundary problems and general domains. The main idea consists of a symmetric extension on the initial domain and the construction of a "control" condition on the extended boundary. That is a restriction of the "source" function generated under conditions in the extended domain that satisfy non-flow conditions on top and bottom of the reservoir.

3. GREEN FUNCTION CONSTRUCTION

In this section we present a mixed boundary value problem and an alternating Schwartz Algorithm in a general form. We assume that the domain Ω is the layer between the planes $x_3 = 0$ and $x_3 = h$ (shown on Figure 3). We further use the notations:

$$\partial\Omega = \Gamma_1 \cup \Gamma_2, \quad \Gamma_2 = \gamma_1 \cup \gamma_2, \quad \text{and} \quad \Gamma_1 \subset \{x \mid 0 < x_3 < h\},$$

where $\gamma_1 = \{x \mid x \in \partial\Omega, x_3 = 0\}$ and $\gamma_2 = \{x \mid x \in \partial\Omega, x_3 = h\}$ are non empty 2-D domains. Let $G(x, \xi)$ be the Green function of the mixed boundary problem (positive solution of the

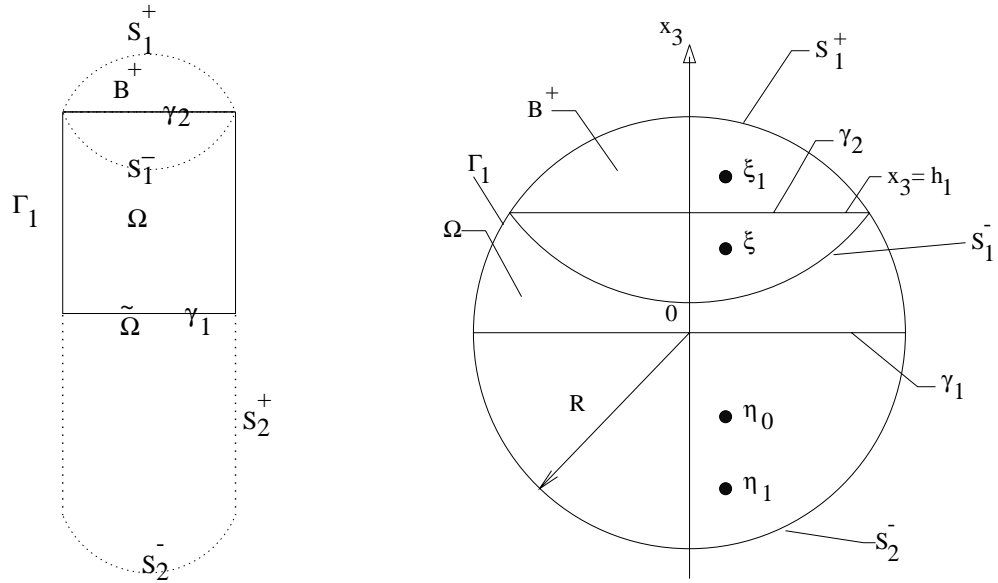


FIGURE 3. Auxiliary domain and its Image: (a) general case; (b) spherical layer with fluxes

problem) with a singularity at ξ :

$$(12) \quad \begin{aligned} \Delta G(x, \xi) &= 0 && \text{in } \Omega \setminus \xi, \\ G_{x_3}(x, \xi) &= 0 && \text{on } \gamma_1, \gamma_2, \\ G(x, \xi) &= 0 && \text{on } \Gamma_1. \end{aligned}$$

3.1. Domain extension (Auxiliary Domains). Assume that there exists symmetric a extension $\tilde{\Omega}$ of the domain Ω with respect to γ_1 such that (see Figure 3(a)):

- $\tilde{\Omega} \cap \{x : 0 < x_3 < h\} \equiv \Omega$;
- there is a sub domain $B^+ \subset \tilde{\Omega}$, symmetric with respect to γ_2 such that

$$\partial B^+ \cap \{x : x_3 > h\} \equiv \partial \tilde{\Omega} \cap \{x : x_3 > h\}.$$

Denote by

$$S_1^+ = \partial B^+ \cap \{x : x_3 > h\} \quad \text{and} \quad S_1^- = \partial \tilde{B}^+ \cap \{x : x_3 < h\}$$

the upper and lower boundaries of the domain B^+ , correspondingly. Further, denote by

$$S_2^+ = \partial \tilde{\Omega} \cap \{x : 0 > x_3 > -h\} \quad \text{and} \quad S_2^- = \partial \tilde{\Omega} \cap \{x : x_3 \leq -h\}$$

the lower and upper boundaries of the extended domain $\tilde{\Omega}$, correspondingly (see, Figure 3(a)).

By construction S_2^+ is a mirror image of Γ_1 , while S_2^- is an mirror image of S_1^+ with respect to the boundary symmetric to γ_1 , and S_2^+ is symmetrical with respect to γ_1 (see Figure 3(a)).

In the case when Ω is a spherical layer, the extension represents itself as a ball and sub domain B^+ is a "lens" (see, Figure 3(b)).

Now assume that $\xi \in \Omega$ is a point of singularity of Green function $G(x, \xi)$. Below we show that for any point ξ there exists a "symmetric" in $\tilde{\Omega}$ and in B^+ finite number of points $A_k(\xi) \in \tilde{\Omega}$ (the extension of the domain Ω), such that:

1. the point $\xi \in A_k(\xi)$;
2. the subset of $A_k(\xi)$ that is in B^+ is symmetric with respect to γ_2 ;
3. the whole set $A_k(\xi)$ is symmetric with respect to γ_1 .

Now, for a given $\xi \in \Omega$ we construct a set with these properties. For simplicity we assume that ξ does not belong to S_1^+ . Take ξ_1 to be the mirror image of ξ with respect to γ_2 . The above assumptions guarantee that such a point exists and is in B^+ . Next, we add to $A_k(\xi)$ the pair of points η_0, η_1 in $\tilde{\Omega}$ that is a mirror image of points ξ, ξ_1 with respect to γ_1 (see Figure 3(b)).

After this step there are three possible cases:

- a:** $\eta_0 \in B^+$ and $\eta_1 \in B^+$;
- b:** $\eta_0 \in B^+$ and $\eta_1 \notin B^+$;
- c:** $\eta_0 \notin B^+$ and $\eta_1 \notin B^+$.

In case (c), we make no additional steps and we consider the set $A_k(\xi)$ constructed and has just these four points. In case (b), we add to $A_k(\xi)$ one point ξ_2 , which is an mirror image of η_0 with respect to γ_2 . Further, we add one more point η_2 which is a mirror image of ξ_2 with respect to γ_1 . In case (a) we add to $A_k(\xi)$ the points ξ_2 and ξ_3 that are a mirror images of the points η_0, η_1 with respect to γ_2 . Then we also add to $A_k(\xi)$ the points η_2 and η_3 that mirror images of ξ_2 and ξ_3 with respect to γ_1 . Further, we repeat the procedure (a)-(c) with respect to the points η_2 and η_3 . Since $h > 0$, after a finite number of steps we reach the case (c) that completes the construction of the set $A_k(\xi)$.

3.2. Alternating Algorithm. In this subsection we present an approximation of the Green function for mixed boundary problem (12). It will be shown that it is a limit of sequence of Green functions of Dirichlet problem in an extended domain with specific condition on its boundary. Let ξ be a point of singularity of the Green Function defined in (12) and let $A_k(\xi)$ be the finite set constructed in Subsection 3.1.

For any $\nu \in A_k(\xi)$ define the Green function $F(x, \nu)$ with zero boundary condition on the extended domain $\tilde{\Omega}$ and with singularity at ν , namely:

$$(13) \quad \begin{aligned} \Delta F(x, \nu) &= 0 & \text{in } \tilde{\Omega} \setminus \nu, \\ F(x, \nu) &= 0 & \text{on } \partial\tilde{\Omega}. \end{aligned}$$

It is a well known fact, that $F(x, \nu)$ can be presented as sums of the fundamental solution of the Laplace equation $\frac{1}{|x-\nu|}$ plus a regular part denoted by $\Phi(x, \nu)$, i.e.

$$(14) \quad F(x, \nu) = \frac{1}{|x-\nu|} + \Phi(x, \nu).$$

In case of standard domain such as cylinder, cube or ball, this function has explicit analytical presentation [7]. Next, we take the superposition of the functions $F(x, \nu)$ in the following form:

$$G_0(x, A_k(\xi)) = \sum_{\nu \in A_k(\xi)} F(x, \nu).$$

It is obvious from the construction that

$$(15) \quad \begin{aligned} \Delta G_0(x, A_k(\xi)) &= 0 & \text{in } \tilde{\Omega} \setminus A_k(\xi), \\ G_0(x, A_k(\xi)) &= 0 & \text{on } \partial\tilde{\Omega}. \end{aligned}$$

Therefore, this is a Green function of the Dirichlet boundary value problem in $\tilde{\Omega}$ with singularities in the set $A_k(\xi)$. Also, by the construction of the set $A_k(\xi)$, the Green function $G_0(x, A_k(\xi))$ is even with respect to γ_1 and therefore it satisfies a homogeneous Neumann boundary condition on γ_1 . Thus, we have the following situation: the restriction of the function $G_0(x, A_k(\xi))$ to the domain Ω is a solution of the Laplace equation with a singularity at the point ξ ; moreover, it satisfies homogeneous Neumann condition on γ_1 and zero Dirichlet boundary condition on Γ_1 . Therefore, $G(x, \xi)$ and $G_0(x, A_k(\xi))$ differ only by the condition on γ_2 . Thus, we consider $G_0(x, A_k(\xi))$ as an approximation to $G(x, \xi)$. Our further steps

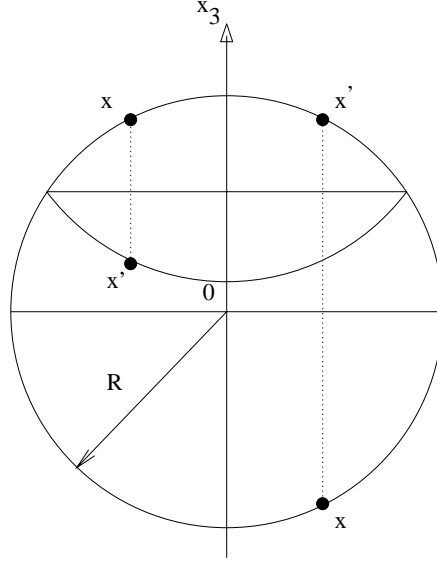


FIGURE 4. Location of the images of the boundary points

will be to correct $G_0(x, A_k(\xi))$ in such a way that they match this boundary condition. This correction is given in the following algorithm:

An Alternating Algorithm:

1. Take the trace of the function $G_0(x, A_k(\xi))$ on S_1^- and denote it by $\phi(x)$.
2. In the domain B^+ find a solution of the problem:

$$(16) \quad \begin{aligned} \Delta g_0(x) &= 0 && \text{in } B^+ \\ g_0(x) &= 0 && \text{on } S_1^- \\ g_0(x) &= \phi(x'(x)) && \text{on } S_1^+, \end{aligned}$$

where $x'(x)$ is a point of S_1^- that is symmetric to the point x on S_1^+ with respect to γ_2 (see, Fig. 4).

3. In the extended domain $\tilde{\Omega}$ find solution to the problem:

$$(17) \quad \begin{aligned} \Delta G_1(x) &= 0 && \text{in } \tilde{\Omega} \\ G_1(x) &= 0 && \text{on } \Gamma_1 \cup S_2^+ \\ G_1(x) &= g_0(x) && \text{on } S_1^+ \\ G_1(x) &= g_0(x'(x)) && \text{on } S_2^-, \end{aligned}$$

where $x'(x)$ is a point on S_2^+ symmetrical to the point x on S_2^- with respect to γ_1 .

Next, we repeat these two steps by replacing $G_0(x)$ by $G_1(x)$ and producing the next pair of functions $g_1(x)$ and $G_2(x)$. Continuing this process, we obtain a sequence of functions $g_0(x), g_1(x), \dots, g_n(x), \dots$ defined in the sub domain B^+ of the extended domain $\tilde{\Omega}$. Also we have obtained the sequence of functions $G_1(x), G_2(x), \dots$ that are even in $\tilde{\Omega}$ with respect to γ_1 . Further denote:

$$\tilde{g}_N(x, \xi) = G_0(x, A_k(\xi)) + g_0(x) + \sum_{n=1}^N [g_n(x) + (G_n(x) - g_{n-1}(x))],$$

and

$$\tilde{G}_N(x, \xi) = G_0(x, A_k(\xi)) + \sum_{n=1}^N G_n(x).$$

The construction guarantees that these functions satisfy the following conditions:

$$(18) \quad \begin{aligned} \Delta \tilde{g}_N(x, \xi) &= 0 && \text{in } B^+ \setminus \xi \\ \tilde{g}_N(x, \xi) &= \tilde{G}_N(x, \xi) && \text{on } S_1^- \\ \tilde{g}_N(x, \xi) &= \tilde{G}_N(x'(x), \xi) && \text{on } S_1^+, \end{aligned}$$

where $x'(x)$ is a point on S_1^+ that is symmetric to x on the S_1^+ with respect to γ_2 ,

$$(19) \quad \begin{aligned} \Delta \tilde{G}_N(x, \xi) &= 0 && \text{in } \tilde{\Omega} \\ \tilde{G}_N(x, \xi) &= 0 && \text{on } \Gamma_1 \cup S_2^+ \\ \tilde{G}_N(x, \xi) &= \tilde{g}_N(x, \xi) && \text{on } S_1^+ \\ \tilde{G}_N(x, \xi) &= \tilde{g}_N(x'(x), \xi) && \text{on } S_2^-, \end{aligned}$$

where $x'(x)$ is a point on S_2^- that is symmetric to the point x on S_1^+ with respect to γ_1 . In the domain B^+ the functions $\tilde{g}_N(x, \xi)$ are even with respect to γ_2 . Similarly, in $\tilde{\Omega}$ the functions $\tilde{G}_N(x, \xi)$ are even with respect to γ_1 . Therefore, the following two conditions are satisfied:

$$(20) \quad (\tilde{g}_N(x, \xi))_{x_3} = 0 \text{ on } \gamma_2,$$

$$(21) \quad (\tilde{G}_N(x, \xi))_{x_3} = 0 \text{ on } \gamma_1.$$

In addition we have:

$$(22) \quad | \tilde{G}_{N+1}(x, \xi) - \tilde{G}_N(x, \xi) | = | \tilde{g}_{N+1}(x, \xi) - \tilde{g}_N(x, \xi) | \text{ on } S_1^+$$

$$(23) \quad | \tilde{g}_{N+1}(x, \xi) - \tilde{g}_N(x, \xi) | = | \tilde{G}_N(x, \xi) - \tilde{G}_{N-1}(x, \xi) | \text{ on } S_1^+.$$

Define:

$$\begin{aligned} M_m(g) &= \max_{S_1^+} | g_{m+1}(x) - g_m(x) |, \\ M_m(G) &= \max_{S_2^-} | G_{m+1}(x) - G_m(x) |, \\ \nu_m(x) &= \frac{G_{m+1}(x) - G_m(x)}{M_m(g)}. \end{aligned}$$

By construction $\nu_m(x)$ satisfies:

$$\Delta \nu_m(x) = 0; \nu_m(x) = 0 \text{ on } \Gamma_1 \cup S_2^+ \text{ and } \nu_m(x) \leq 1 \text{ on } S_1^+ \cup S_2^-.$$

By the assumption S_1^- and $\partial \tilde{\Omega}$ intersect at non zero angle so we can apply the lemma (see, e.g. [9] Chapter 4.4), to function $\nu_m(x)$. This lemma implies that

$$(24) \quad | \nu_m(x) | \leq q < 1 \text{ on } S_1^-.$$

At the same time on S_1^- , by construction :

$$\nu_m(x) = \frac{g_{m+1}(x) - g_m(x)}{M_m(g)}.$$

Combined with (24), this implies that:

$$M_{m+1}(g) \leq q M_m(g).$$

Further, we construct $M_m(G)$ in a similar way. As a result, we obtain sequences $\{M_m(g)\}$ and $\{M_m(G)\}$ that converge to zero at a rate of geometric progression with ratio q . Hence, there exist the limits:

$$\lim_{m \rightarrow \infty} \tilde{g}_m(x, \xi) = \tilde{g}(x, \xi) \text{ in } B^+, \text{ and } \lim_{m \rightarrow \infty} \tilde{G}_m(x, \xi) = \tilde{G}(x, \xi) \text{ in } \tilde{\Omega}.$$

On γ_1 the functions $\tilde{G}_N(x, \xi)$ satisfy the condition $(\tilde{G}_N(x, \xi))_{x_3} = 0$ for any N (by the symmetry property (21)). Therefore, their limit $\tilde{G}(x, \xi)$ satisfies homogeneous Neumann condition on γ_1 . On γ_2 , by the construction, $\tilde{g}_N(x, \xi)$ has the same property, i.e. $(\tilde{g}_N(x, \xi))_{x_3} = 0$. Also, by construction, $\tilde{G}_N(x, \xi) - \tilde{g}_N(x, \xi) = 0$ on S_1^+ and on S_1^- the difference

$$\tilde{G}_N(x, \xi) - \tilde{g}_{N-1}(x, \xi) = \tilde{G}_N(x, \xi) - \tilde{G}_N(x, \xi)$$

approaches zero. Then limits $\tilde{G}(x, \xi)$ and $\tilde{g}(x, \xi)$ are equal in B^+ , so that by (20) $(\tilde{G}(x, \xi))_{x_3} = 0$ on γ_2 as well. QED.

Possible Generalization:

All construction which is done for Laplace equation could be generalized on elliptic operator of second order in divergence with bounded and measurable coefficients. This type of equation models fluid filtration in highly heterogeneous anisotropic porous media. Namely let

$$(25) \quad L = \sum_{i,j}^3 \frac{\partial}{\partial x_i} (k_{i,j}(x) \frac{\partial}{\partial x_j})$$

For applying this technique the coefficients of the operator L in (25) should be extended evenly on extended domain $\tilde{\Omega}$. Let coefficients $\tilde{k}_{i,j}$ of extended elliptic operator \tilde{L} be such that

$$\tilde{k}_{i,j} = k_{i,j} \text{ in } \Omega$$

$$\tilde{k}_{i,j} - \text{ is an even function with respect } \gamma_2 \text{ in } B^+$$

$$\tilde{k}_{i,j} - \text{ is an even function with respect } \gamma_1 \text{ in } \tilde{\Omega}$$

All construction for Green function of mixed boundary problem 12 for operator \tilde{L} in the extended domain are justified as well for Laplace equation. Differences concern only main estimation (24), that is based on Lemma from Chapter 4.2 of [9]. Instead this Lemma we can for example apply more general proposition for so called L-harmonic measure obtained in [12].

4. NUMERICAL IMPLEMENTATION OF THE METHOD

In Subsection 2.3 we proposed an approximation method for solving the problem (6) - (8). The essence of the method was to approximate the potential (9) by (10). In the previous section we provided a method for computing the Green function $G(x, \xi)$. Our construction ensures that on the boundary $\partial\Omega$ the function $G(x, \xi)$ satisfies the conditions (8). The main task in this section is to provide an approximation to the equation (11). This will lead to a linear system for the discrete densities β_i . First, we present an algorithm for computing an approximation to $G(x, \xi)$. The ball B is considered as a symmetric extension of the layer Ω . Therefore, the Green function in the formulae (10) could be represented as a limit of the sequence $\{\tilde{G}_N(x, \xi)\}$. Note, that for obtaining functions $\tilde{G}_N(x, \xi)$ it is not required to solve the problems in the lens B^+ . The $\tilde{G}_N(x, \xi)$ can be represented as a sum:

$$(26) \quad \tilde{G}_N(x, \xi) = G_0(x, A_k(\xi)) + \sum_{n=1}^N \Pi_n(x, \xi),$$

So that by (14) $G_0(x, \xi)$ has the form

$$(27) \quad G_0(x, \xi) = \sum_{\nu \in A_k(\xi)} \left\{ \frac{1}{|x - \nu|} + \Phi(x, \nu) \right\},$$

where $\Phi(x, \nu)$ is the regular part of the Green function in the ball B (see, e.g. [7]). The Π_n in (26) is the Poisson operator

$$(28) \quad \Pi_n(x, \xi) = (4\pi)^{-1} \int_{\partial B} \frac{(R^2 - |x|^2)\phi_n(y)}{R|x - y|^3} dS_y,$$

with

$$(29) \quad \phi_n(y) = \begin{cases} \tilde{g}_n(y), & \text{on } S_1^+, \\ 0, & \text{on } \Gamma_1 \cup S_2^+, \\ \tilde{g}_n(y'), & \text{on } S_2^-. \end{cases}$$

Here, the functions $\tilde{g}_n(y)$ have been defined in the same way as in Section 3.2 for the the domain $\tilde{\Omega} = B$; also point y' in (29) is given by the construction in step 2 of the *alternating algorithm* (see, Figure 4). The Poisson integral (28) could be calculated by a Simpson-type cubature formulae [1]. Some practical computations performed in [13] have shown that for $R = 5000m$, $h = 10m$ a cubature with 4040 nodes guarantees an accuracy 10^{-4} of the normal derivative of $\tilde{G}_N(x, \xi)$ on γ_2 for $N = 5$ steps (explained in Subsection *Alternating Algorithm*). The Simpson formula gives higher accuracy but is quite expensive. In our calculation we have used a less accurate but very efficient Lusternik formula [1] with 64 nodes. Further, in order to find the discrete densities β_i we need to compute integrals of the Green function over Δ_i . This step is implemented in following way: Using presentation (26) of $\tilde{G}_N(x, \xi)$ and formulae (27) for $G_0(x, A_k(\xi))$ the integral over Δ_i in (10) is presented in the form:

$$\int_{\Delta_i} \tilde{G}_N(x, \xi) d\xi = \int_{\Delta_i} \left\{ F_N(x, \xi) + \sum_{\nu \in A_k(\xi)} \left[\frac{1}{|x - \nu|} + \Phi(x, \nu) \right] \right\} d\xi,$$

where $F_N(x, \xi) = \sum_{n=1}^N \Pi_n(x, \xi)$ is a regular function.

In our numerical implementation the last two integrals are calculated analytically while the first one is computed numerically. Thus, the outer problem is solved numerically on any step of the iteration process described in Subsection 5.1. For this purpose at any step the computed integrals can be substituted in the equation (11) as an approximation of the pressure function and radial rate(4). Then numerical values of β_i are obtained by Gauss method as a solution of linear $N \times N$ system equation(11) derived for the collocation points. Results of the computations for β_i , $i = 1, \dots, 3000$ in two cases are presented on Figure 5 . In our computations $L = 2000m$, $r_w = 0.075m$, and $r_w = 0.05m$. The hydrodynamic meaning of discrete density distribution is a local influx towards the well surface. And it is clear from this picture how the conjugate flow in the reservoir/well system effects the distribution of local flux along the well. Namely: when the radius of the well, r_w , decreases, then the resistance to the flow in the well increases. Therefore, the local influx takes its maximum near $x_1 = 0$, the dominated end of the well. At the same time at the free end of the well, $x_1 = L$, the influx is reduced. Near the end points $x = 0$ and $x = L$ we see certain spikes in the behavior, called "end effects".

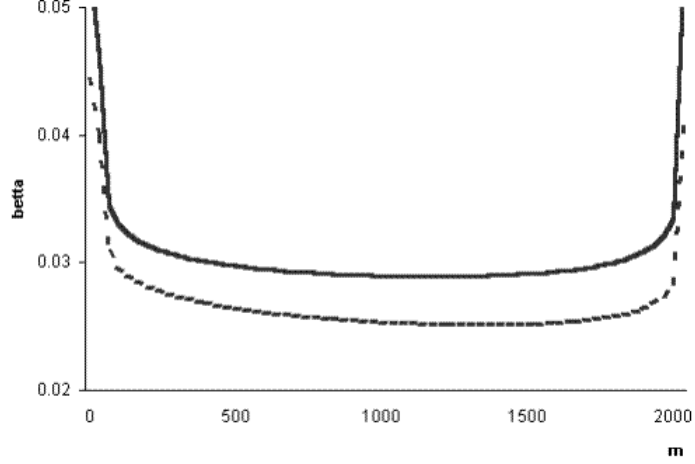


FIGURE 5. Comparison of local flux vs wells radius($r_w = 0.075m$ dotted line, $r_w = 0.05m$ continuous line)

4.1. Computational Results and Discussion. As noted above, an interesting fact is the dependence of the pressure drop and local production distribution along the well on geometrical parameters of reservoir/well system.

It has been shown [2], that in an unbounded 3-D porous media with "normal permeability" (less than 1D) and for flows obeying conditions 1-6 in section 2.1, the pressure drop along the well-bore is insignificant. In a bounded reservoir the dependence on geometrical parameters could lead to a significant pressure drop. For examine the impact of geometrical characteristics of the reservoir boundary on production rate and pressure drop is the aim of this section. Here the variable parameters are: L - length of the well, D_b - distance between free end of the well and reservoir boundary, location of the dominated end of the well, r_w - well's radius, shape of the reservoir boundary namely $1/R$ -radius of the curve of the ball $B(0, R)$.

1. First we examine the influence of the shape factor of the reservoir. Our computations show that the pressure drop along the well-bore depends essentially on the form of the exterior boundary Γ_1 . The results for two limiting cases (spherical and plane external boundaries) are given in Figure 6. Here $\langle P \rangle = \frac{1}{\pi r^2 L} \int_L P_a(x_1) dx_1$ is the average pressure in the well-bore and P_w is the pressure at the fixed (dominated) end. In both cases the distance between free end and the external boundary remained the same. These results show, that boundary shape could lead up to 10% increase of pressure drop.
2. Next we analyzed the impact of the distance between well and reservoir exterior boundary Γ_1 on the pressure drop in the well. It is clear that if the free end of the well intersects with the reservoir external boundary, the pressure drop is equal to the difference between pressure on the dominated end and the value of pressure on external boundary pressure. We studied the influence of the D_b on a value of the pressure at the free end of the well on. In computational runs it was assumed that well length L , reservoir's radius R_b , well radius r_w and well location x_3^0 with respect to top and bottom, are constant. So the parameter D_b decreases while shifting of the well towards Γ_1 . The corresponding results are presented on Figure 7. Here P_L is the pressure at the free end of the well-bore. As may be seen from Figure 7 this relation is not significant for small D_b (about $20r_w$). But when the free end of the well is close enough to the external boundary the pressure at this end decreases exponentially. Note that the increase of well length, which does not

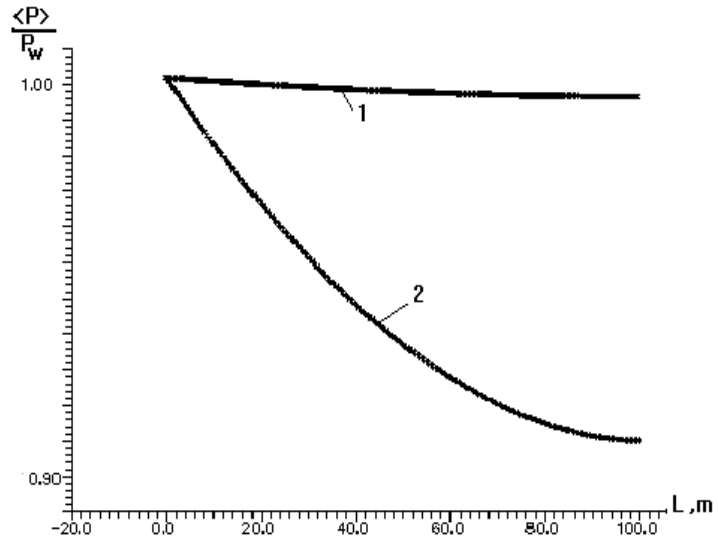


FIGURE 6. Distribution of the $\langle P \rangle$ within a well in reservoir with plane 1 and spherical 2 external boundary

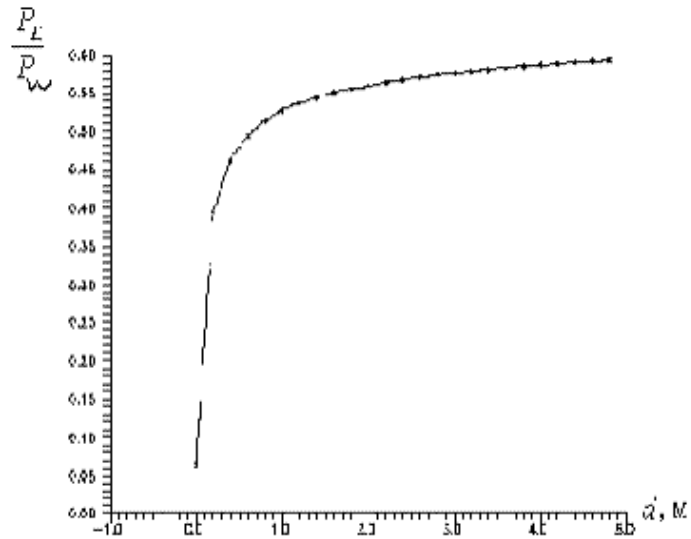


FIGURE 7. Ratio between P_L and P_w vs distance to exterior boundary

decreases the distance D_b , also causes considerable pressure drop at the free end of the well. For this purpose the following numerical experiment has been executed.

3. Take the distance D_b , well radius r_w , and R_b are constant and vary parameter was the L length of the well.

The results of numerical experiments showed that the influence of the dominated end of the well on the free end of the well could decrease even proportionally to the well length.

4. It is known from field data [10], [20] that as a result of pressure drop along the well the dependence of production rate on the well length tends to be constant. So, the

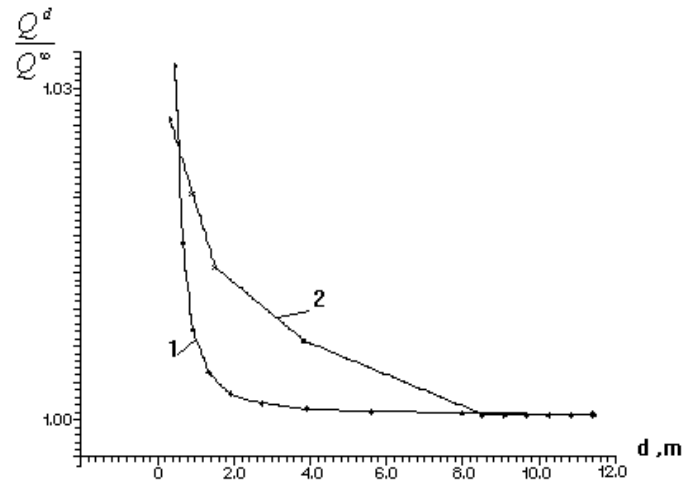


FIGURE 8. Comparison of the relation between production rate vs. distance to the exterior boundary

correlation between the production rate of the horizontal well has been studied for two cases: (a) constant pressure in the well, and (b) variable pressure in the well generated by reservoir/well flux.

We have assumed that the length L , the well location x_3^0 with respect to top and bottom and radius r_w remain constant. The variable parameter is D_b . As shown on Figure 8, in case of constant pressure the production rate sharply decreased and stabilized as the distance from the reservoir boundary increased. In case of variable pressure in the hole, the curve is much smoother.

5. As noted above the shape of the reservoir could result in substantial changes of the pressure drop. In the model considered a quantitative characteristics of the shape of the reservoir boundary is the curvature radius $R_e = \frac{1}{R_b}$. Using our model the influence of the R_e on the well production rate has been evaluated. A series of computations with constant length L , radius of the well r_w , and distance D_b has been computed. The variable parameter was R_e . The corresponding results is illustrated on Figure 9. According to these computations there exist such a critical value R_e^0 , depending on L and D_b , that if R_e is larger than this critical value R_e^0 then the production rate would no longer depend on R_e . It is important to note that all these results were obtained for abnormally high permeability values ($k = 10D$), very short distances (10 m) to the external reservoir boundary and big enough radius of the well (0.1 m). We wanted to show that the proposed method could be used to estimate the effects of the geometry on the production rate and the pressure distribution along the well-bore. When the distance to the external boundary and the reservoir permeability were chosen more realistically, the picture is similar but the pressure drop is significantly smaller. Thus, we came to the same conclusion as in [2], that within the considered assumption there are no limitations on the length of horizontal well imposed by its hydrodynamics effectiveness. At the same time it is well known that the hydro dynamical resistance of a pipe strongly depends on its radius.
6. The impact of the well bore radius on the pressure drop along the well has been studied further. The results of the computations of cases that satisfy the assumption (1) - (8)

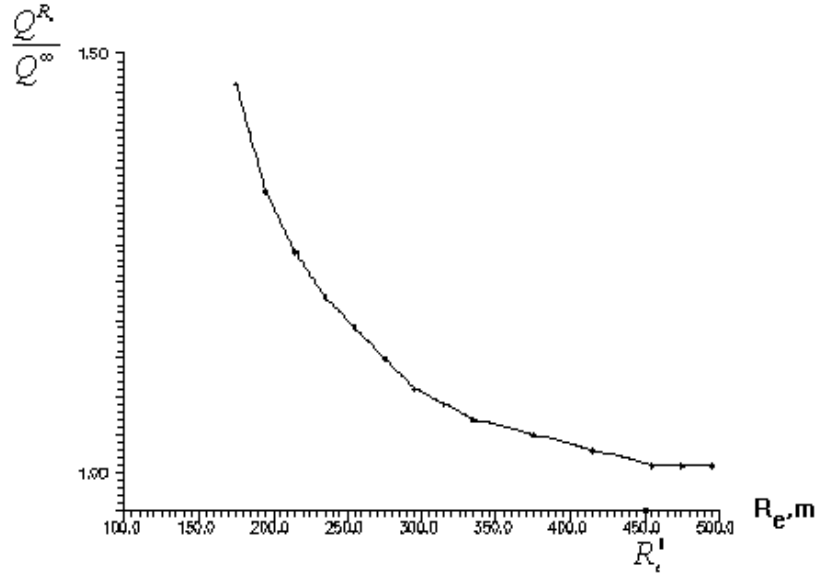


FIGURE 9. Production rate vs. reservoir curvature

in subsection 2.1 are presented on Figure 10. In these computations we varied the well radius r_w , and fixed the $R_b = 10000$ m, $k = 100$ MD, $D_b = 100$ m, and $L = 1000$ m. As shown on Figure 10, the pressure drop in a well of very small radius may reach tens of percents.

High-pressure drops in a long horizontal well may thus be accounted for by different technological reasons (such as well completion, casing/tubing diameters, sand factor, screen permeability etc.) resulting in a decrease of the actual diameter of bore-hole. Therefore, it is important to study the impact of the actual radius of the well on the flow along the well. The distribution of local influx along the well for two cases are presented on the Figure 11. These results show that well radius could substantially reduce the local flux towards the well. In these computations $L = 2000$ m. The number of discretizations along the well is equal 3000.

In the next section another model and method that can take into account the impact of wells of finite conductivity on the pressure drop are presented.

5. COUPLED POROUS MEDIA MODEL

In this section the well is modeled as a super-collector, that is porous media with extremely high permeability. We assume that the well and the reservoir are cylinders and the flows are coupled through their interface. The corresponding mathematical problems are solved by the method of separation variables and the solutions are represented in the form of Fourier-Bessel series [7]. In order to describe our model we need some notations. The well and the reservoir are represented by the domains W and Ω , correspondingly:

$$W \equiv A_0 \cup A_1, \text{ where}$$

$$A_0 \equiv \{x : x_2^2 + x_3^2 < r_0^2; 0 < x_1 < L\}; \quad A_1 \equiv \{x : r_0^2 < x_2^2 + x_3^2 < r_w^2; 0 < x_1 < L\},$$

and

$$\Omega \equiv A_2 + A_3, \text{ where}$$

$$A_2 \equiv \{x : r_w^2 < x_2^2 + x_3^2 < R_b^2; 0 < x_3 < H; 0 < x_1 < L\};$$

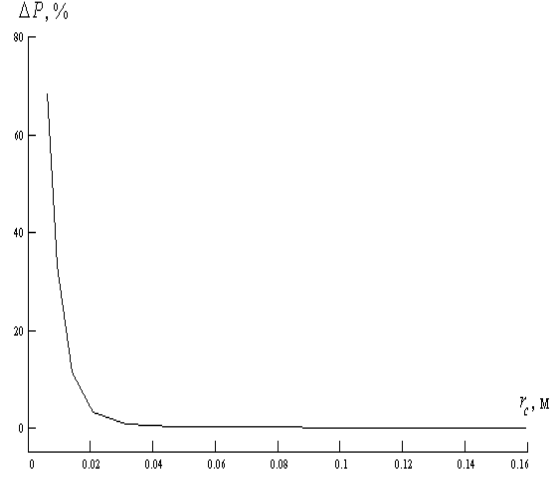


FIGURE 10. Pressure drop along the well-bore vs bore-hole radius

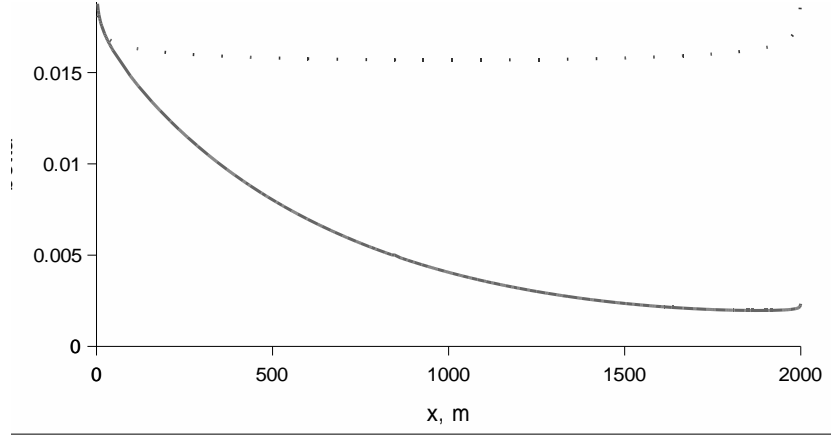


FIGURE 11. Local flux towards well ($r_w = 0.025m$ -continuous line $r_w = 0.1m$)

$$A_3 \equiv \{x : x_2^2 + x_3^2 < r_w^2; 0 < x_3 < H, L < x_1 < H\}.$$

Here $x = (x_1, x_2, x_3)$ are the Cartesian coordinates of the points x in the reservoir. One of the possible ways to couple the flows in the regions W and Ω , A_0 , A_1 , A_2 , A_3 is the following:

1. A_0 is the well tubing or more general - oil or gas transport domain, where flow is subjected to the approximation of pipe hydrodynamics;
2. A_1 is the well annuli (screen between tubing and casing) or more general - “super collector”, a bottom hole zone with small diameter with high permeability k_1 , where flow satisfies Darcy law;
3. $A_2 + A_3$ represents the reservoir itself (bounded by the top ($y = H$) and the bottom ($y = h$)) with permeability k_2 .

This domain contains two boundaries of discontinuity of the media:

- ∂A_0 , the boundary between tubing and bottom hole zone of porous media, where the conjugate condition (6) is satisfied.
- ∂A_1 , the boundary between “super collector” and porous media of the reservoir.

Thus we consider the model:

1. The average pressure $P_a(x_1)$ satisfies equations (3) in A_0 , conjugate boundary conditions (6) on the well surface $x_2^2 + x_3^2 = r_w^2$ and the condition (5) on the free end of the well $x_1 = L$,
2. The pressure $p(x)$ satisfies the Laplace equation In A_1 , A_2 and A_3 ;
3. On the interfaces between domains A_1 , A_2 and A_3 the pressure and the normal component of the velocity are continuous.

Analytical solution of this general problem could be developed by using iterative techniques. First, one can apply the developed technique for spherical layer Ω in the Section 2 to cylindrical domain and show the following:

Let $\tilde{\Omega}$ is a cylindrical extension of the domain Ω . There exists a pressure distribution on the external boundary of the extended domain $\tilde{\Omega}$, such that the solution of the problem in a cylinder annuli $\tilde{\Omega}$ with this boundary condition will satisfy non-flow conditions on the top and the bottom.

Thus, one can reduce the problem to the following two step procedure:

1. **First step:** Split the cylinder $\tilde{\Omega}$ into four homogeneous media, i.e. $\tilde{\Omega} = \tilde{A}_2 \cup A_1 \cup A_0 \cup A_3$, where

$$\tilde{A}_2 \equiv \{x : r_w^2 < x_2^2 + x_3^2 < R_b^2; 0 < x_1 < L\}.$$

2. **Second step:** Solve the two problems in the cylinder $A = A_0 \cup A_1 \cup \tilde{A}_2$ and A_3 , correspondingly by a non-overlapping domain decomposition algorithm [6, 29].
3. **Third step:** Reduce the problem in A to a sequence of problem in A_0 and $B = A_1 + \tilde{A}_2$. This sequence is linked through conjugate condition (6) and converges as a geometrical progression.

Finally, the overall problem is reduced to the problem of flow with mixed boundary conditions in heterogeneous porous media in an annulus cylinder B with permeability

$$(30) \quad K = \begin{cases} k_1 & \text{in } A_1, \\ k_2 & \text{in } \tilde{A}_2. \end{cases}$$

Detailed description of the proposed methods is beyond the scope of the present paper. Here we will cover part of the algorithm that gives the analytical solution of the mixed boundary problem in highly heterogeneous porous media $B = A_1 + \tilde{A}_2$. The algorithm is realized in the form of a Fourier-Bessel series. It makes possible to investigate explicitly the dependence of the pressure drop on the well radius (casing/tubing diameter) and well/reservoir conductivity ratio.

5.1. Splitting of the problem. We introduce new variables $x = x_1/r_w, y = x_2/r_w, z = x_3/r_w, r^2 = x_2^2 + x_3^2; z = z$ then the main dimensionless geometrical parameters are : $L = l/r_w, R_0 = r_0/r_w, R = R_b/r_w$. Domains B, A_1 and \tilde{A}_2 are transformed into:

$$A_1 = \{(r; z) : R_0 < r < 1; 0 < z < L\} \text{ and } A_2 = \{(r; z) : 1 < r < R; 0 < z < L\}.$$

$$B = \{(r; z) : R_0 < r < R; 0 < z < L\}$$

Define the edge and lateral parts of the cylindrical domains A_1, A_2 as follows (see Figure 12):

$$a_1 = \{R_0 < r < 1, z = 0\}; b_1 = \{R_0 < r < 1, z = L\}; c_1 = \{r = R_0, 0 < z < L\},$$

$$a_2 = \{1 < r < R, z = 0\}; b_2 = \{1 < r < R, z = L\}; c_2 = \{r = R, 0 < z < L\}.$$

Denote the interface between A_1 and A_2 as $d = \{r = 1; 0 < z < L\}$. Further, we make the following assumptions:

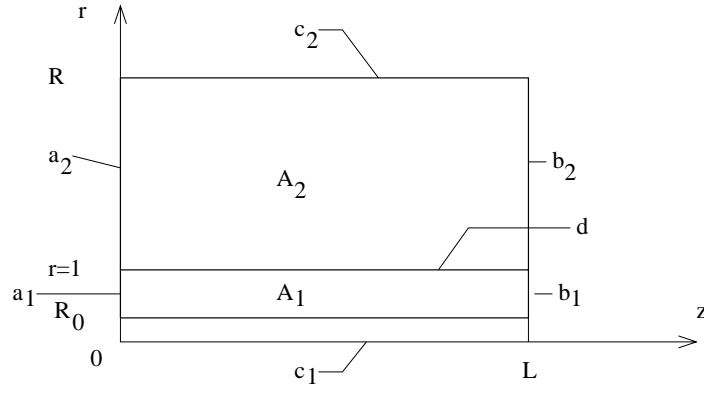


FIGURE 12. Scheme of cylindrical reservoir

1. we have Darcy flow in B with discontinuous permeability (30);
2. the pressure p and radial component of the velocity are continuous at the interface d between A_1 and A_2 ;
3. the pressure is given on the boundary a_1 and equals to p_w ;
4. a non flow condition is specified on a_2 ;
5. the reservoir pressure p_b on the right end, and on the external boundary b_1 , b_2 , and c_2 of the cylinder is given;
6. pressure is a linear function of z along the boundary c_1 ; that corresponds to Poiseil flow in the tubing of the well (more general distribution could be considered in the same way as in previous section).

Thus for reduced pressure function

$$(31) \quad \bar{p} = (p - p_b)/(p_w - p_b) = \begin{cases} p_1 & \text{in } A_1 \\ p_2 & \text{in } A_2. \end{cases}$$

we obtain following mixed boundary-value problem:

$$(32) \quad \begin{aligned} \Delta p_1 &= 0 && \text{in } A_1 \\ p_1 &= 1 && \text{on } a_1 \\ p_1 &= 1 - z/L && \text{on } c_1 \\ p_1 &= 0 && \text{on } b_1 \end{aligned}$$

$$(33) \quad \begin{aligned} \Delta p_2 &= 0 && \text{in } A_2 \\ (p_2)_z &= 0 && \text{on } a_2 \\ p_2 &= 0 && \text{on } c_2 \\ p_2 &= 0 && \text{on } b_2 \end{aligned}$$

The coupling conditions on the interface d between the media A_1 and A_2 are following:

$$(34) \quad p_1|_{r=1-0} = p_2|_{r=1+0}$$

$$(35) \quad k_1 \frac{\partial p_1}{\partial r} \Big|_{r=1-0} = k_2 \frac{\partial p_2}{\partial r} \Big|_{r=1+0}$$

The method, the algorithm, and the main results presented bellow remain the same for any type of Dirichlet or Neumann conditions on external the boundary of the annular cylinder B namely on a_1 , a_2 , b_1 , b_2 , c_2 .

5.2. Alternating algorithm without overlapping. In this sub section modification of Schwarz Dirichlet-Neumann [29] alternating algorithm without overlapping in coupling cylindrical annuli is presented. If the ratio $G = k_2/k_1$ is very small then the pressure in the reservoir (domain A) is close to discontinuous function that is a linear function in A_1 and equals to zero in A_2 . When G increases then the pressure might be adjusted both in A_1 and in A_2 so it becomes smoother. Moreover, it is obvious that the increase of G decreases the pressure in A_1 and increases the pressure A_2 . Under the assumption that $G = k_2/k_1 < 1$ this process is implemented as an iterative procedure:

1. At each step solve two problems: (a) (33) in the domain A_2 with homogeneous Dirichlet condition on the interface d ; (b) (32) in the domain A_1 with homogeneous Neumann conditions on the same side.
2. Extend this solution through the interface between A_1 and A_2 . The extension is subject to the coupling conditions (34),(35);
3. Correct this extension on non-joint parts of a boundary.

A distinctive feature of this process is the correction of the solution only on non-joint part of boundary: $a_1, a_2, b_1, b_2, c_1, c_2$, because on the interface d between A_1 and A_2 the pressure and the normal flux satisfy the coupling conditions on each step automatically.

From a mathematical point of view this iterative procedure makes possible to represent the solution of the problem (32), as a sum of three types of functions: $U_i(r, z)$, $W_i(r, z)$ and $V_i(r, z)$, where $U_0(r, z) = (L - z)/L$, $W_0(r, z)$ and $V_0(r, z)$ are equal zero, and for $i = 1, 2, \dots$ the functions $U_i(r, z)$, $W_i(r, z)$ and $V_i(r, z)$ are solutions to the following problems:

- (1) Function $U_i(r, z)$ is a solution of the problem

$$(36) \quad \begin{aligned} \Delta U_i(r, z) &= 0 \text{ in } A_1 \cup A_2 \\ U_i(R_0, z) = U_i(r, 0) &= 0 \\ \frac{\partial U_i(1, z)}{\partial r} &= 0 \\ U_i(r, 0) &= -V_i(r, 0) - W_i(r, 0), \text{ when } R_0 < r < 1. \end{aligned}$$

- (2) Function $V_i(r, z)$ is a solution of:

$$(37) \quad \begin{aligned} \Delta V_i(r, z) &= 0 \text{ in } A_1 \cup A_2 \\ V_i(1, z) = V_i(R, z) &= 0 \\ V_i(r, 0) &= 0, \\ (V_i(r, 0))_z &= -(U_{i-1}(r, 0))_z \end{aligned}$$

Moreover, function $V_i(r, z)$ have to satisfies the coupling conditions (34,35).

Then each function

$$(38) \quad \mathcal{V}_N = \sum_{i=1}^N (U_i + V_i)$$

for $N \geq 1$ satisfies all boundary conditions except the condition on c_1 and c_2 . Thus, we introduce the following correction:

(3) Function $W_i(r, z)$ is a solution of the problem

$$(39) \quad \begin{aligned} \Delta W_i(r, z) &= 0 \\ W_i(R, z) &= -U_{i-1}(R, z) \\ W_i(r, L) &= 0 \\ W_i(1-0, z) &= W_i(1+0, z) \\ W_i(R_0, z) &= -V_i(R_0) \text{ on } c_1. \end{aligned}$$

In next subsection 5.3 it will be shown that functions: $U_i(r, z)$, $W_i(r, z)$ and $V_i(r, z)$, exist and can be represented in the form of Fourier and Fourier-Bessel series. Moreover, we find a condition on the parameters G and R/R_0 , (but not on the length L !), so that $V_i(r, z)$ tends to zero with rate of geometric progression with a ratio $q < 1$.

Then the function

$$(40) \quad u_N = U_0 + V_N + \sum_{i=1}^N W_i$$

by the construction solution of Laplace equation in A_1 and A_2 and satisfies all boundary conditions in the problems (32-33), except conditions on c_1 and c_2 . Function u_N on c_1 is equal to $(L-z)/L + V_N(R_0, z)$ on c_1 and $1 + V_N(r, 0)$ on a_1 and in addition $V_N(r, z)$ tends to zero when N tends to ∞ . Thus, u_N tends to the solution of the problem (32)-(35).

Presentation (40) contains main pressure function U_0 generating flow in the pipe (solution of the problem (3)-(5)) and the sum of terms generated by perturbations of the reservoir's flux. These "flux" terms dominate in case when the parameter coefficient of heterogeneity G is near one and are negligible when G is small.

5.3. Implementation of non-overlapping Algorithm. The first approximation U_0 is a linear function: $U_0 = (L-z)/L$ and it satisfies all conditions except two boundary conditions:

$$\text{on } a_2 \text{ when } z = 0, 1 < r < R \text{ and on } c_2 \text{ when } r = R, 0 < z < L.$$

To correct the function U_0 on a_2 and on c_2 we solve the the problem (37). The solution of this problem is sought in form of Fourier-Bessel series [7]: $V_i = \Phi_i(r, z)$ in A_2 , and $V_i = G\Phi_i(r, z)$ in A_1 . Here

$$(41) \quad \Phi_i(r, z) = \sum_{m=1}^{\infty} R_m(r) D_m(i) \frac{\sinh(\nu_m z)}{\nu_m \cosh(\nu_m L)},$$

$$(42) \quad R_m(r) = J_0(\nu_m r) Y_0(\nu_m) - J_0(\nu_m) Y_0(\nu_m r),$$

Where ν_m is the root of the equation $R_m(R) = 0$.

The $D_m(1)$ in (41) is a Fourier-Bessel coefficient of the function $-1/L$. The function $U_0 + V_1$ satisfies all conditions (33-35) except the conditions on a_1, c_1 and c_2 . To correct it we need to solve the the problems (36) and (39) with corresponding boundary conditions on a_1 and c_1 . The solutions U_i can be represented in the form:

$$(43) \quad U_i(r, z) = \sum_{k=1}^{\infty} C_k(i) E_k(r) \frac{\sinh(\mu_k z)}{\sinh(\mu_k L)}$$

Here $E_k(r) = J_0(\mu_k r) Y_0(\mu_k R_0) - J_0(\mu_k R_0) Y_0(\mu_k r)$ and μ_k is a root of the equation $E_k(\mu_k) = 0$; $C_k(i)$ are Fourier-Bessel coefficients of the function $G\Phi_i(r, L)$. An application of the maximum

principle gives the following inequality:

$$(44) \quad C_k(i) \leq C_k^*(i), \quad \text{where } C_k^*(i+1) = -GC_k^*(i) \sum_{m=1}^{\infty} g_m Q_m.$$

Here

$$Q_m = \frac{2}{1-R_0} \int_{R_0}^1 r R_m(r) dr \quad \text{and} \quad g_m = \frac{\pi J_0(\nu_m R)}{J_0(\nu_m) + J_0(\nu_m R)}.$$

Assume that G , R and R_0 are such that

$$(45) \quad G \sum_1^{\infty} Q_m g_m \leq q < 1.$$

Then from the recurrence relation (44) it follows that $C_k(i) \leq q^i$. Finally, we have to make the last correction concerning the conditions on the sides c_1 and c_2 of annuli cylinder. For this purpose we have already introduced the problem (39). The solution of this problem has the form:

$$\begin{aligned} W_i(r, z) &= \sum_{n=1}^{\infty} R_n^1(r, z) \cos(B_n z) && \text{in } A_1 \\ W_i(r, z) &= \sum_{n=1}^{\infty} R_n^2(r, z) \cos(B_n z) && \text{in } A_2 \\ R_n^1 &= a_n^1 I_0(B_n r) + a_n^2 K_0(B_n r) \\ R_n^2 &= b_n^1 I_0(B_n r) + b_n^2 K_0(B_n r) \\ a_n^1 I_0(B_n) + a_n^2 K_0(B_n) &= b_n^1 I_0(B_n) + b_n^2 K_0(B_n) \\ a_n^1 I_1(B_n) - a_n^2 K_1(B_n) &= G(b_n^1 I_1(B_n) - b_n^2 K_1(B_n)) \\ a_n^2 K_0(B_n R_0) &= f_n^1 - a_n^1 I_0(B_n) \\ b_n^1 I_0(B_n R) &= f_n^2 - b_n^2 K_0(B_n R). \end{aligned}$$

Here $B_n = \frac{\pi(2n+1)}{2L}$, f_n^1 is the Fourier coefficient of $V_i(R_0, z)$, and f_n^2 is the Fourier coefficient of $U_{i-1}(R, z)$. Then the function

$$u_N = \sum_{i=1}^N U_i(r, z) + \sum_{i=1}^N V_i(r, z) + \sum_{i=1}^N W_i(r, z)$$

satisfies all conditions except the conditions on $z = L$, $1 < r < R$, where $U_N(r, L)$ tends to zero because of condition (45) Q.E.D.

Conclusions:

1. The actual ratio reservoir/well conductivity has a greater impact on the pressure drop as compared to other parameters of the system "reservoir + horizontal well". Second in significance parameter influencing the pressure drop is the radius of the well.
2. The ratio reservoir/well conductivity is defined by the completion of the well (tubing radius, actual "screen + sand pack" conductivity etc.) and actual radius of oil/gas flow along the tubing.
3. When the ratio of reservoir/well conductivity is very small ($G = \frac{k_2}{k_1} \ll 1$), then the productivity index of horizontal well is significantly affected by the geometrical parameters of the reservoir. From our results it can be deduced in the case $G \ll 1$ that: the distance from the external boundary on the first place, the shape factor (curvature of the reservoir boundary) on the second place, and length of the well in third place affect the pressure drop along the well.

4. Because of the pressure drop along the well-bore, the productivity of the horizontal well, beginning at certain critical value ceases to grow with increase of its length. The proposed computational methods can be used to predict accurately this critical length and its dependence on ratio reservoir/well conductivity.

List of used notations

μ	–	<i>viscosity</i>
K	–	<i>permeability</i>
p	–	<i>pressure in the reservoir</i>
r_w	–	<i>radius of the well</i>
L	–	<i>length of the well</i>
P_a	–	<i>average pressure in the well – bore</i>
P_w	–	<i>pressure in the fixed (dominated) end of the well</i>
P_L	–	<i>pressure on the free boundary of the well</i>
D_b	–	<i>distance between free boundary of the well and reservoir boundary</i>
R	–	<i>radius of external boundary</i>
h	–	<i>reservoir thickness</i>
$R_e = 1/R$	–	<i>curvature radius of external boundary (shape factor)</i>
$B(0, R)$	–	<i>sphere of radius R</i>
r_0	–	<i>casing radius</i>
r^2	–	$x^2 + y^2$
$J_0(Y_0)$	–	<i>Bessel function of zero order of first (second) kind</i>
$I_0(K_0)$	–	<i>Modified Bessel functions of zero order of first (second) kind</i>

REFERENCES

- [1] Abramowitz, M., Stegun, I., *Handbook of Mathematical Function*, Dover Publication, New York, 1965.
- [2] Antipov, D.M., Ibragimov, A.I., and Panfilov, M.B., Model of Coupled Fluid Flow in a Reservoir and Inside a Horizontal Well, *Fluid Dynamics*, **31** (1996).
- [3] Azar-Nejad, F., Tortike, W.S., and Faroug-Ali, S.M., 3-D Analytical Solution of the Diffusivity Equation with Application to the Horizontal Wells, *SPE 35512 1996 European 3D Modeling Conference* (April, 1996), Stavanger, Norway.
- [4] Aziz, K. and Setari, A., *Petroleum Reservoir Simulation*, Applied Science, New York, 1979.
- [5] Borisov, J.P., Pilatovsky, V.P., and Tabakov, V.P., *Oil Production Using Horizontal and Multiple Deviation Wells*, Nedra, in Russian, Moscow, 1964.
- [6] Bramble J., Pasciak J.E., and Schatz A., The construction of preconditioners for elliptic problems by sub-structuring. I-IV, *Math. Comp.*, **47**, **49**, **51**, **53** (1986)-(1989), 103-134, 1-16, 415-430, 1-24.
- [7] Budak, B.M., Samarsky, A.A., Thichonov, A.A., *A Collection of Problems in Mathematical Physics*, Dover Publication, New York, 1988.
- [8] Cinco, L.H., Samaniego-V.F., Dominguez, N., Transient Pressure behavior for well With Finite-Conductivity Vertical Fracture, *SPEJ*, **18** (August 1978), 253.
- [9] Courant, R., *Partial Differential Equations*, New York, London, 1962.
- [10] Dikken B.J., Pressure Drop in Horizontal Wells in Horizontal Well and Its Effects on Production Performance *JPT*, **1426** (1990).
- [11] Ewing, R., Ibragimov, A., Lazarov, R., 3-D Simulation of the pressure drop along Horizontal Wells in a Bounded Reservoir, *SPE Intern. Conf. on Horizontal Well Technology*, (November 2000) Calgary, Canada.
- [12] Ibragimov, A., Landis, E., *Applicable AnalySis*, **67** (1997), 269–282.
- [13] Ibragimov, A.I., and Necrasov, A.A., An Analogue of Schwarz Method for Construction of the Green’s Function for Zaremba’s Problem, *Journal of Computational Mathematics and Mathematical Physics* **38** (1998).
- [14] Ibragimov, A Baganova, M., Necrasov, A., Domain Decomposition Methods and There Application to Modeling of the Performance of Horizontal and Slanting Wells in the Anisotropic Reservoir *SPE 51906 Reservoir Simulation Symposium*, February 1999, Houston.
- [15] Ibragimov, A.I. Baganova, M.N., Necrasov, A.A., Stationary and Non-stationary Flow of Fluid in a Limited Towards Horizontal and Slanting Wells, *SPEJ 97-132, Special Edition*, **38** (1999).
- [16] Joshi, S.D., *Horizontal Well Technology*, Pen-Well Publishing Company, Tulsa, 1991.
- [17] *Journal of Canadian Petroleum Technology*, Special edition 1999, **38** (1999).
- [18] Musket M., *Under Ground Hydrodynamic*, Dover Publication, New York, 1965.

- [19] Nekrasov A.A., Simulation conjugate flow gas-condensate mixture in reservoir and inside horizontal well, *Gas Industry* **1-2** (1996).
- [20] Novy, R.A., Pressure Drop in Horizontal Well: When Can They be Ignored, *SPE* (February 1995) **29**, Trans AIME, 299.
- [21] Ouyang, L., Arabi, F., Aziz K., General Well-Bore Flow Model for Horizontal, Vertical and Slanted Well Completion, *71 SPE Annular Technical Conference and Exhibition, 1996*, Denver, Colorado.
- [22] Ouyang, L., Thomas, L., Evanse, C., Aziz, K., Simple but Accurate Equations for Well-bore Pressure Draw-down Calculation, *SPE 38314 SPE Western Regional Meeting* (1997), Long Beach, California.
- [23] Ouyang, L., Aziz, K., A Simulation Approach to Couple Well-bore Flow and R reservoir Inflow for Arbitrary Well Configurations *SPE 48936, Annual Technical Conference, September 1998*, New Orleans, Louisiana.
- [24] Ozgan, E., et al, Effect of Conductivity on Horizontal-Well Pressure Behavior, *SPE Advanced technology Series* (March 1995) 85.
- [25] Ozgan, E., Sarica, A., Haci, M., Influence of Pressure Drop Along the Well-bore on Horizontal-Well Productivity, *SPEJ* (September 1999), 288.
- [26] Panfilov M.B, Equations of motion of a viscous fluid in a horizontal well *Information Review of VNIEGazprom. Gas and Gas-condensate Field Development*, Moscow, Russia, **1** (1993).
- [27] Peaceman, D.W., Interpretation of Well-block Pressure in Numerical Reservoir Simulation, *JPT* **18** (June, 1978).
- [28] *Proceedings of SPE Intern. Conf. on Horizontal Well Technology*, (November 2000), Calgary, Canada.
- [29] Quarteroni A., *Domain Decomposition Method for Partial Differential Equations*, Oxford: Calderon Press; New York, Oxford University Press, 1999.
- [30] Renato, A., Economides, M.J., Performance of Multiple Horizontal Well in Low to Medium-permeability Reservoirs, *SPE, Reservoir Engineering*, (May 1996).